A General and Parallel Platform for Mining Co-Movement Patterns over Large-scale Trajectories

ABSTRACT

1. INTRODUCTION

The prevalence of positioning devices has drastically boosted the scale and spectrum of trajectory collection to an unprecedented level. Tremendous amounts of trajectories, in the form of sequenced spatial-temporal records, are continually generated from animal telemetry chips, vehicle GPSs and wearable devices. Data analysis on large-scale trajectories benefits a wide range of applications and services, including traffic planning [1], animal analysis [2], and social recommendations [3], to name just a few.

A crucial task of data analysis on top of trajectories is to discover co-moving patterns. A *co-movement* pattern [4] refers to a group of objects traveling together for a certain period of time and the group is normally determined by spatial proximity. A pattern is prominent if the size of the group exceeds M and the length of the duration exceeds K, where M and K are parameters specified by users. Rooted from such basic definition and driven by different mining applications, there are a bunch of variants of co-movement patterns that have been developed with more advanced constraints.

Table 1 summarizes several popular co-moving pattern s with different constraints in the attributes of clustering in spatial proximity, consecutiveness in temporal duration and computational complexity. In particular, the *flock* [5] and the *group* [6] patterns require all the objects in a group to be enclosed by a disk with radius r; whereas the *convoy* [7], the *swarm* [8] and the *platoon* [9] patterns resort to density-based spatial clustering. In the temporal dimension, the *flock* [5] and the *convoy* [7] require all the timestamps of each detected spatial group to be consecutive, which is referred to as *global consecutiveness*; whereas the *swarm* [8] does not impose any restriction. The *group* [6] and the *platoon* [9] adopt a compromised manner by allowing arbitrary gaps between the consecutive segments, which is called *local consecutiveness*. They introduce a parameter L to control the minimum length of each local consecutive segment.

Patterns	Proximity	Consecutiveness	Time Complexity
flock [10]	disk-based	global	$O(|\mathbb{O}||\mathbb{T}|(M + log(|\mathbb{O}|)))$
convoy [7]	density-based	global	$O(|\mathbb{O}|^2 + |\mathbb{O}||\mathbb{T}|)$
swarm [8]	density-based	-	$O(2^{|\mathbb{O}|}|\mathbb{O}||\mathbb{T}|)$
group [6]	disk-based	local	$O(|\mathbb{O}|^2|\mathbb{T}|)$
platoon [9]	density-based	local	$O(2^{|\mathbb{O}|}|\mathbb{O}||\mathbb{T}|)$

Table 1: Constraints and complexity of co-movement patterns. The time complexity indicates the performance in the worst case, where $|\mathbb{O}|$ is the total number of objects and $|\mathbb{T}|$ is the number of descritized timestamps.

Figure 1 is an example to demonstrate the concepts of various co-movement patterns. The trajectory database consists of six moving objects and the temporal dimension is discretized into six snapshots. In each snapshot, we treat the clustering methods as a black-box and assume that they generate the same clusters. Objects in proximity are grouped in the dotted circles. As aforementioned, there are three parameters to determine the co-movement patterns and the default settings in this example are $M = 2$, $K = 3$ and $L = 2$. Both the *flock* and the *convoy* require the spatial clusters to last for at least K consecutive timestamps. Hence, $\{o_3, o_4\}$ and $\{o_5, o_6\}$ remains the only two candidates matching the patterns. The *swarm* relaxes the pattern matching by discarding the temporal consecutiveness constraint. Thus, it generates many more candidates than the *flock* and the *convoy*. The *group* and the *platoon* add another constraint on local consecutiveness to retain meaningful patterns. For instance, $\{o_1, o_2 : 1, 2, 4, 5\}$ is a pattern matching local consecutiveness because timestamps $\{1, 2\}$ and $\{4, 5\}$ are two segments with length no smaller than $L = 2$. The difference between the *group* and the *platoon* is that the *platoon* has an additional parameter K to specify the minimum number of snapshots for the spatial clusters. This explains why $\{o_3, o_4, o_5 : 2, 3\}$ is a *group* pattern but not a *platoon* pattern.

As can be seen, there are various co-movement patterns requested by different applications and it is cumbersome to design a tailored solution for each type. In addition, despite the generality of the *platoon* (i.e., it can be reduced to other types of patterns via proper parameter settings), it suffers from the so-called *loose-connection* anomaly. We use two objects o_1 and o_2 in Figure 2 as an example to illustrate the scenario. These two objects form a *platoon* pattern in timestamps $\{1, 2, 3, 102, 103, 104\}$. However, the two consecutive segments are 98 timestamps apart, resulting in a false positive co-movement pattern. In reality, such an anomaly may be caused by the periodic movements of unrelated ob-
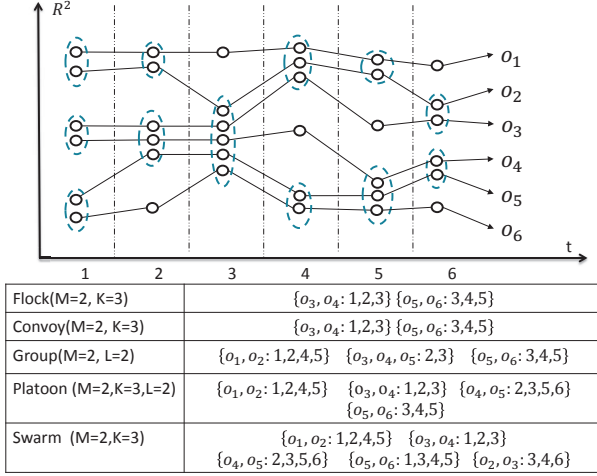
Figure 1: Trajectories and co-movement patterns; The example consists of six trajectories across six snapshots. Objects in spatial clusters are enclosed by dotted circles. M is the minimum cluster cardinality; K denotes the minimum number of snapshots for the occurrence of a spatial cluster; and L denotes the minimum length for local consecutiveness.

Flock(M=2, K=3)	$\{o_3,o_4:1,2,3\}\{o_5,o_6:3,4,5\}$
Convoy(M=2, K=3)	$\{o_3,o_4:1,2,3\}\{o_5,o_6:3,4,5\}$
Group(M=2, L=2)	$\{o_1,o_2:1,2,4,5\}$ $\{o_3,o_4,o_5:2,3\}$ $\{o_5,o_6:3,4,5\}$
Platoon (M=2,K=3,L=2)	$\{o_1,o_2:1,2,4,5\}$ $\{o_3,o_4:1,2,3\}$ $\{o_4,o_5:2,3,5,6\}$ $\{o_5,o_6:3,4,5\}$
Swarm (M=2,K=3)	$\{o_1,o_2:1,2,4,5\}$ $\{o_3,o_4:1,2,3\}$ $\{o_4,o_5:2,3,5,6\}$ $\{o_5,o_6:1,3,4,5\}$ $\{o_2,o_3:3,4,6\}$

jects, such as vehicles stopping at the same petrol station or animals pausing at the same water source. Unfortunately, none of the existing patterns have directly addressed this anomaly.
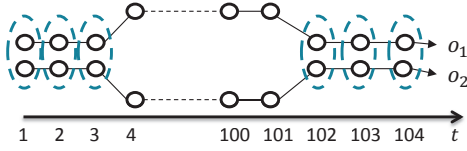

Figure 2: *Loose-connection* anomaly. Even though $\{o_1, o_2 : 1, 2, 3, 102, 103, 104\}$ is considered as a valid *platoon* pattern, it is highly probable that these two objects are not related as the two consecutive segments are 98 timestamps apart.

The other issue with existing methods is that they are built on top of centralized indexes which may not be scalable. Table 1 shows their theoretical complexities in the worst cases and the largest real dataset ever evaluated in previous studies is up to million-scale points collected from hundreds of moving objects. In practice, the dataset is of much higher scale and the scalability of existing methods is left unknown. Thus, we conduct an experimental evaluation with 4000 objects moving for 2500 timestamps to examine the scalability. Results in Figure 3 show that their performances degrade dramatically as the dataset scales up. For instance, the detection time of *group* drops twenty times as the number of objects grows from *1k* to *4k*. Similarly, the performance of *swarm* drops over fifteen times as the number of snapshots grows from *1k* to *2.5k*. These observations imply that existing methods are not scalable to support large-scale trajectory databases.

Therefore, our primary contributions in this paper are to close these two gaps. First, we propose the *general co-movement pattern* (GCMP) which models various co-moment patterns in a unified way and can avoid the *loose-connection*
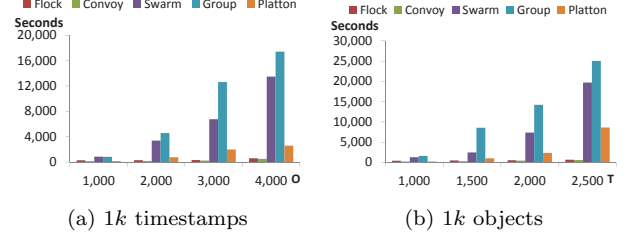

(a) $1k$ timestamps (b) $1k$ objects

Figure 3: Performance measures on existing co-movement patterns. A sampled Geolife data set is used with up two 2.4 million data points. Default parameters are $M = 10$ $K = 20$ $L = 10$.

anomaly. In GCMP, we introduce a new gap parameter G to pose a constraint on the temporal gap between two consecutive segments. By setting a feasible G, the loose-connection anomaly can be avoided. In addition, our GCMP is both general and expressive. It can be reduced to any of the previous patterns by customizing the parameters.

Second, we investigate deploying our GCMP detector on MapReduce platforms (such as Hadoop and Spark) to tackle the scalability issue. Our technical contributions are three-fold. First, we replicate the snapshots in multiple data chunks to support efficient parallel processing. Second, we devise a novel *Star Partition and Mining* (SPM) algorithm as a fine-granularity partitioning strategy to achieve workload balance. For each star, an Apriori method is adopted to mine the co-movement patterns. Third, we propose two types of optimization techniques to further improve the performance, including *edge-simplification* to boost the shuffle process and *temporal monotonicity pruning* and *forward closure checking* to significantly reduce the number of enumerated candidates in the Aproiro algorithm.

We conduct a set of extensive experiments on XXX datasets with billion-scale trajectory points. The results show that XXX.

The rest of our paper is organized as follows: Section 2 summarizes the relevant literature on trajectory pattern mining. Section 3 states the problem definition of our general co-movement pattern mining. Section 4 provides a naive *temporal replication and mining* solution. An advanced solution named *star partition and mining* is presented in Section 5. Section 6 discusses various optimization techniques. Section 7 conducts extensive experiments to verify the usefulness and efficiency of our system. Finally Section 8 concludes the paper.

2. RELATED WORKS

The *co-movement patterns* in literature consist of five members, namely *group* [6], *flock* [10], *convoy* [7], *swarm* [8] and *platoon* [9]. We have demonstrated the semantics of these patterns in Table 1 and Figure 1. In this section, we focus on comparing the techniques used in these works. For more trajectory patterns other than *co-movement patterns*, interested readers may move to [11] for a comprehensive survey.

2.1 Flock and Convoy

The difference between *flock* and *convoy* lies in the object clustering methods. In *flock* objects are clustered based on their distance. Specifically, the objects in the same cluster

needs to have a pair-wised distance less than *min_dist*. This essentially requires the objects to be within a disk-region of delimiter less than *min_dist*. In contrast, *convoy* cluster the objects using density-based clustering [12]. Technically, *flock* utilizes a mth-order Voronoi diagram [13] to detect whether a subset of object with size greater than m stays in a disk-region. *Convoy* employs a trajectory simplification [14] technique to boost pairwise distance computations in the density-based clustering. After clustering, both *flock* and *convoy* use a line-sweep method to scan each snapshots. During the scan, the object group appears in consecutive timestamps is detected. Meanwhile, the object groups that do not match the consecutive constraint are pruned. However, such a method faces high complexity issues when supporting other patterns. For instance, in *swarm*, the candidate set during the line-sweep grows exponentially, and many candidates can only be pruned after the entire snapshots are scanned.

2.2 Group, Swarm and Platoon

Different from *flock* and *convoy*, all the *group,swarm* and *platoon* patterns have more constraints on the pattern duration. Therefore, their techniques of mining are of the same skeleton. The main idea of mining is to grow object set from an empty set in a depth-first manner. During the growth, various pruning techniques are provided to prune unnecessary branches. *Group* pattern uses the Apriori property among patterns to facilitate the pruning. *Swarm* adapts two more pruning rules called backward pruning and forward pruning. *Platoon* further adapts a prefix table structure to guide the depth-first search. As shown by Li et.al. [9], *platoon* outperforms other two methods in efficiency. However, the three patterns are not able to directly discover the general co-movement pattern. Furthermore, their pruning rules heavily rely on the depth-first search nature, which lost its efficiency in the parallel scenario.

2.3 MaReduce Framework

MapReduce (MR) was formally proposed by Dean et.al. [15] and has subsequently implemented by many open source systems. Those systems provide handy APIs with fault tolerances and are popularly used as large-scale data processing platforms. In simple words, there are two conceptual types of computing nodes in MR, namely the *mapper*s and the *reducer*s. The execution of a MR algorithm consists of three major steps: First, input data are partitioned and read by a *map* function on each mapper. Then, mappers emit key-value pairs which are *shuffle*d over the network to reducers. Lastly, reducers process the received data using a *reduce* function.

3. DEFINITIONS

Let $\mathbb{O} = \{o_1, o_2, ..., o_n\}$ be the set of objects and $\mathbb{T} = \{1, 2, ..., m\}$ be the descritized temporal dimension. A time sequence T is defined as a subset of $\mathbb{T}$, i.e., $T \subseteq \mathbb{T}$, and we use $|T|$ to denote sequence length. Let T_i be i-th entry in T and we say T is consecutive if $\forall 1 \leq i \leq |T|-1, T_{i+1} = T_i+1$. It is obvious that any time sequence T can be decomposed into consecutive segments and we say T is *L-consecutive* [9] if the length of all the consecutive segments is no smaller than L.

As illustrate in Figure 2, patterns adapting the notion of *L*-consecutiveness (e.g., *platoon* and *group*) still suffer from

Pattern	M	K	L	G	Clustering
Group	2	1	2	$|\mathbb{T}|$	Disk-based
Flock	·	·	K	1	Disk-based
Convoy	·	·	K	1	Density-based
Swarm	·	·	1	$|\mathbb{T}|$	Density-based
Platoon	·	·	·	$|\mathbb{T}|$	Density-based

Table 2: Expressing other patterns using GCMP. · indicate a user specified value. M represents the object *size* constraints. K represents *duration* constraint. L represents *consecutiveness* constraint. G represents the *connection* constraints.

loose connection problem. To avoid such an anomaly without losing pattern generality, we introduce a parameter G to control the gaps between timestamps in a pattern. Formally, a G-connected time sequence is defined as follows:

Definition 1 (G-connected). *A time sequence T is G-connected if the gap between any of its neighboring timestamps is no greater than G. That is $\forall T_i, T_{i+1} \in T, T_{i+1} - T_i \leq G$.*

We take $T = \{1, 2, 3, 5, 6\}$ as an example, which can be decomposed into two consecutive segments $\{1, 2, 3\}$ and $\{5, 6\}$. T is not 3-consecutive since the length $\{5, 6\}$ is 2. Thus, it is safe to say either T is 1-consecutive or 2-consecutive. On the other hand, T is 2-connected since the maximum gap between its neighboring time stamps is $5 - 3 = 2$. It is worth noting that T is not 1-connected because the gap between T_3 and T_4 is 2 (i.e., 5-3=2).

Given a trajectory database descritized into snapshots, we can conduct a clustering method, either disk-based or density-based, to identify groups with spatial proximity. Let T be the set of timestamps in which a group of objects O are clustered. We are ready to define a more general co-movement pattern:

Definition 2 (General Co-Movement Pattern). *A general co-movement pattern finds a set of objects O satisfying the following five constraints: 1) closeness: the objects in O belong to the same cluster in the timestamps of T; 2) significance: $|O| \geq M$; 3) duration: $|T| \geq K$; 4) consecutiveness: T is L-consecutive; and 5) connection: T is G-connected.*

There are four parameters in our general co-movement pattern, including object constraint M and temporal constraints K, L, G. By customizing these parameters, our pattern can express other patterns proposed in previous literature, as illustrated in Table 2. In particular, by setting $G = |T|$, we achieve the *platoon* pattern. By setting $G = |T|, L = 1$, we achieve the *swarm* pattern. By setting $G = |T|$, $M = 2$, $K = 1$, we gain the *group* pattern. Finally by setting $G = 1$, we achieve the *convoy* and *flock* pattern. In addition to the flexibility of representing other existing patterns, our GCMP is able to avoid the *loose connection* anomaly by tuning the parameter G. It is notable that GCMP cannot be modeled by existing patterns.

It is also observable that the number of patterns in GCMP could be exponential under some parameter settings (i.e., when expressing *swarm*). In particular, given a parameter M, if a pattern P is valid, then any subset of P with size M is also a valid pattern. This results in additional $\Sigma_{M \geq i \geq |P.O|} \binom{|P.O|}{i}$ patterns, which is clearly overwhelming and redundant. For all these patterns, output P is sufficient.

Therefore, we define the *Closed General Co-Movement Pattern* as follows:

Definition 3 (Closed General Co-Movement Pattern). *A general co-moving pattern $P = \langle O : T \rangle$ is closed if and only if there does not exist another general co-moving pattern P' s.t. $P.O \subseteq P'.O$.*

For example, let $M = 2, K = 2,, L = 1, G = 1$. In Figure 1, the pattern $P_1 = \{o_3, o_4 : 1, 2, 3\}$ is not a closed pattern. This is because $P_2 = \{o_3, o_4, o_5 : 2, 3\}$ is a closed pattern since $P_2.O \supset P_1.O$. The closed pattern avoids outputting duplicate information, thus making the result patterns more compact.

Our definition of GCMP is free from clustering method. Users are able to supply different clustering methods to facilitate different application needs. We currently expose both disk-region based clustering and DBSCAN as options to the user.

In summary, the goal of this paper is to present a parallel solution for discovering closed GCMP from large-scale trajectory data.

Before we move on to the algorithmic part, we list the notations that are used in the following sections.

Symbols	Meanings
Tr_i	trajectory of object i
S_t	snapshot of objects at time t
$\mathbb{O}$	set of objects
M	object size constraint
K	duration constraint
L	consecutiveness constraint
G	connection constraint
$P = (O : T)$	pattern with object set O, time sequence T
$C_t(o)$	the cluster of object o at time t
Sr_i	the star of object i

Table 3: Symbols and notions that will be used

4. TEMPORAL REPLICATION AND MINING

We resort to the MapReduce (MR) paradigm for designing a scalable parallel solution in mining GCMP. It is straightforward to partition the trajectory database into equal-sized temporal segments; and then mining the GCMP patterns out of each segments. However, GCMP patterns may cross multiple temporal segments. To ensure the correctness, we need to guarantee that every valid pattern can be mined within at least one partitions. Thus, some snapshots need to be replicated several times in multiple partitions. This leads us to design the *Temporal Replication and Mining* (TRM) algorithm.

The work flow of TRM is illustrate as in Figure 4. In brief, there are two pipeline MR jobs which further consist of four stages. The first MR job is considered as a preprocessing, where input trajectories are grouped into snapshots and each snapshot runs a clustering method (e.g., Disk-based, DB-SCAN, etc.). The output is shown as in Figure 4(b). The second MR job is the *TRM* algorithm. In the *map* phase (i.e., Figure 4 (c)), temporally closed snapshots are grouped into a partition. In the *reduce* phase (i.e., Figure 4 (d)), a *Line Sweeping* method is developed to discover GCMP in

each partition. Finally, patterns from different partitions are then collected to form the final output.

In the first MR job, each partition contains only one snapshot for clustering, thus it is unnecessary to replicate any snapshots. Therefore, we focus on describing the second MR job which is the *Temporal Replication and Mining* algorithm. We use η to denote the replication factor. The outline of TRM is shown in Algorithm 1.

Algorithm 1 Temporal Replication and Mining

Require: list of $\langle t, S_t \rangle$ pairs
1: $\eta \leftarrow (\lceil \frac{K}{L} \rceil - 1) * G + 2K - 2$
2: —Map Phase—
3: **for all** $\langle t, S_t \rangle$ **do**
4:      **for all** $i \in 1...R$ **do**
5:          emit a $\langle t - i, S_t \rangle$ pair
6:      **end for**
7: **end for**
8: —Partition and Shuffle Phase—
9: **for all** $\langle t, S \rangle$ pair **do**
10:      group-by t, emit a $\langle t, Par_t \rangle$
11:      where $Par_t = \{S_t, S_{t+1}, ..S_{t+R}\}$
12: **end for**
13: —Reduce Phase—
14: **for all** $\langle t, Par_t \rangle$ **do**
15:      lineSweepMining(Par_t)
16: **end for**

As shown in Algorithm 1, the TRM algorithm contains three steps. First, in the map phase, each snapshot is keyed with its timestamp (lines 2-7). Second, in the partition phase, every snapshot is grouped with its next η snapshots to form a partition (lines 8-12). Third, in the reduce phase, a line sweeping method is invoked to mine GCMP within each partition (lines 13-15). It is easy to see that this method replicates a snapshots at most η times. The replication factor η is critical for the performance of TRM. If the η is large, the shuffle cost as well as the reduce cost would be high. On the contrary, if η is small, valid patterns may be missed out. In the Algorithm 1, the η is chosen as $(\lceil \frac{K}{L} \rceil - 1) * G + 2K - 2$. We will shortly show that this is the minimum η to guarantee the correctness.

4.1 Line Sweep Mining

Each task in the reduce phase processes a partition Par_i, which contains η snapshots starting from snapshot S_i. We observe that within each Par_i, only the patterns whose object sets are contained in the first snapshot are necessary to be reported. Therefore, we design a simple *line-sweep mining*(LSM) method for discovering GCMPs. The algorithm works as in Algorithm 2.

The algorithm scans snapshots in a partition in sequence. During the scan, it maintains a candidate set C which contains potential patterns (line 1). The algorithm starts by inserting clusters at S_i to C (lines 2-4). Subsequently, in each iteration, clusters in C are joined with clusters at S_i to generate a new set of patterns N(lines 6). The valid new patterns form a new candidate set C and any invalid patterns are discarded(lines 8 and 11).

4.2 Correctness of TRM

We prove the correctness of TRM in three aspects. First, setting $\eta = (\lceil \frac{K}{L} \rceil - 1) * G + 2K - 2$ would not miss any
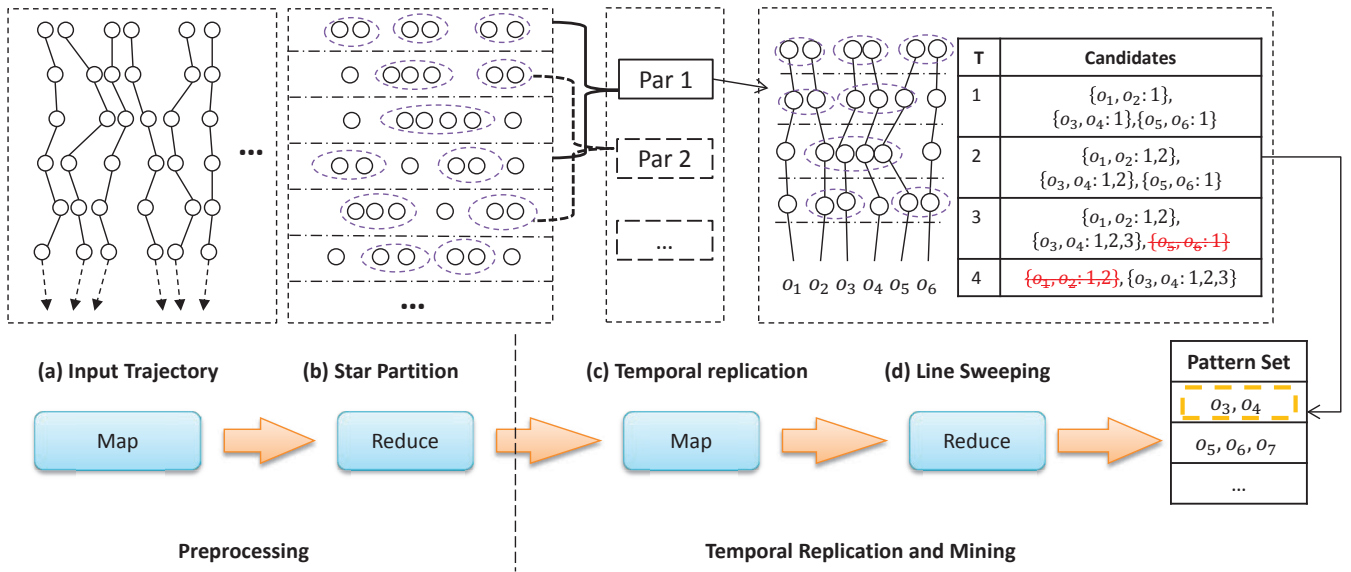
Figure 4: Work flow of Temporal Replication and Mining. (a)(b) correspond to the first MR job which computes the clusters at each snapshot; (c)(d) correspond to the second MR job which uses TRM to mine GCMP in parallel.

Algorithm 2 Line Sweep Mining

Require: $Par_t = \{S_t, S_{t+1}, ...\}$
1: $C \leftarrow \{\}$ ▷ Candidate set
2: **for** $c \in S_t$ **do**
3:      C.add($\langle c, t \rangle$)
4: **end for**
5: **for all** $i \in [1, R]$ **do**
6:      $N \leftarrow S_{t+i} \oplus C$
7:      **for all** $n \in N$ **do**
8:          **if** $|n.O| \geq M$ **then** C.add(n).
9:          **end if**
10:      **end for**
11:      remove unqualified candidate from C
12: **end for**
13: output qualified candidate in C

---

valid patterns. Second, no false patterns are reported in any partitions. Third, the choice of η is minimum. We formalize the first two properties as *completeness* and *soundness* as follows:

Definition 4 (Completeness and Soundness). *Let a partition method $\mathbb{P}$ partitions a trajectory database Tr into segments, $Par_1, ..., Par_m$. $\mathbb{P}$ is complete if for every valid pattern P in Tr, $\exists Par_i$ s.t. P is valid in Par_i. $\mathbb{P}$ is sound if for all patterns that are valid in any Par_i, they are also valid in Tr.*

Apparently, in TRM, replicating the entire trajectories (i.e., $\eta = |\mathbb{T}|$) meets the *soundness* and *completeness* requirements. However, it burdens the network shuffle and limits the parallelism. We prove in the following theorem that the minimum η is $(\lceil \frac{K}{L} \rceil - 1) * G + 2K - 2$ to ensure the correctness:

Theorem 1 (Correctness of Temporal Replication). *The minimum η to ensure sound and complete of the temporal replication is $(\lceil \frac{K}{L} \rceil - 1) * G + 2K - 2$.*

Proof. The soundness of partition can be observed from the fact that each partition represents a consecutive segments of trajectories. Therefore patterns in a partition can be directly mapped back to original trajectories. For completeness, let T' be the *shortest* valid subsequence (wrt. K, L, G) of a valid sequence T. Let η be the upper bound for all T's among all possible valid sequence. It is easy to see that, under such a setting, any valid sequence would be captured by one of the partitions in temporal replication. This proves the completeness. Now, we compute the minimum value of η as follows: any T' can be viewed as n consecutive segments with sizes $l_1, .., l_n$ and $n-1$ gaps with sizes $g_1, ..., g_{n-1}$. Since η is the upper bond among all T's, η can be formulated as follows:

$$\eta = \max_{n, l_i, g_i} \{\Sigma_{i=1}^{i=n} l_i + \Sigma_{i=1}^{i=n-1} g_i\} \qquad (1)$$

With the following constraints: $(1) \forall l_i, L \leq l_i \leq K - 1; (2) \forall g_i, 1 \leq g_i \leq G; (3) \Sigma_{i=1}^{i=n} l_i \geq K$ and $(4) \Sigma_{i=1}^{i=n-1} l_i \leq K - 1$. The constraint $(1)(2)(3)$ due to the validity of T' and the constraint (4) is because of the minimum size of T'. Observe that, constraints (1)-(4) form a convex polygon and η is monotone increasing wrt. n, l_i, g_i, the maximum value of η is thus taken at the boundaries. Further observe that $n \in [2, \lceil \frac{K}{L} \rceil]$ and $K \geq 1$, these conditions naturally derive $\eta = (\lceil \frac{K}{L} \rceil - 1) * G + 2K - 2$. $\square$

Example 1. *We illustrate the work flow of TRM method using Figure 4 (c)(d) with $M = 2, K = 3, L = 2, G = 2$. In Figure 4 (c), snapshots are combined into partitions with sizes equal to $(\lceil \frac{K}{L} \rceil - 1) * G + 2K - 2 = 4$. Then a line sweep method is performed in (d) for partition 1. Each C_i refers to the candidate set during sweeping snapshot i. Initially, C_1 contains patterns whose object set is in snapshot 1. As line sweeps, at snapshot 3, since the timestamps of $\{o_5, o_6\}$ is $\{1\}$, which violates both the L, and G constraints, this candidate is eliminated. At snapshot 4, since the timestamps of $\{o_1, o_2\}$ is $\{1, 2\}$, which violates the L constraints, thus it is*

5

removed. Therefore, $\{o_3, o_4\}$ is the qualified pattern and is outputted.

The TRM approach though achieves good parallelism, it requires to replicate the data η times. In the cases of *swarm*, *group* and *platoon*, η meeds to be as large as $|\mathbb{T}|$. Handling those cases are equivalent to replicate the entire snapshots to each partition, which surrenders the benefit of parallelism.

5. STAR PARTITION AND MINING

TRM approach requires to replicate entire trajectories $O(|\mathbb{T}|)$ times, which is inefficient in parallelism. To overcome this limitation, we propose the *Star Partition and Mining* (SPM) method. In SPM, we design a graph model, named *connection graph*, to capture the co-moving behavior among objects. In such a way, given an object u, all the objects potentially co-moved with u are captured in u's neighborhood, which forms a *star* structure in graph terms. SPM utilizes such structures to partition objects and then adapts an Apriori algorithm to discover true GCMPs from each partition.

The flow of SPM method is presented in Figure 5. SPM utilizes the same preprocessing as TRM, thus the flow starts from clusters in each snapshot. Conceptually, the clusters in each snapshot forms a graph as shown in Figure 5 (a). In the map phase of *SPM*, a vertex together with its neighborhood vertexes form a star. Every star is indeed an independent partition. Then, stars are shuffled to reducers. As in Figure 5 (c), Apriori mining algorithm is adapted to mine the GCMP patterns. The overview implementation of SPM is shown in Algorithm 3.

Algorithm 3 Star Partition and Mining

Require: list of $\langle t, S_t \rangle$ pairs
1: —Map phase—
2: **for all** $C \in S_t$ **do**
3:     **for all** $(o_1, o_2) \in C \times C$ **do**
4:         **if** $o_1 < o_2$ **then**
5:             emit a $\langle o_1, o_2, \{t\} \rangle$ triplet
6:         **end if**
7:     **end for**
8: **end for**
9: —Partition and Shuffle phase—
10: **for all** $\langle o_1, o_2, \{t\} \rangle$ triplets **do**
11:     group-by o_1, emit $\langle o_1, Sr_{o_1} \rangle$
12: **end for**
13: —Reduce phase—
14: **for all** $\langle o, Sr_o \rangle$ **do**
15:     Apriori(Sr_o)
16: **end for**

5.1 Star Partition

The intuition of the star partition is that, if two objects are part of the same pattern, they must belong to the same cluster at those snapshots. Therefore, we may link objects that belong to the same cluster to form the *connection graph*. Objects that are not connected surely fail to form a pattern. We may then partition the connection graph based on vertex connectivity such that mining GCMPs can be done in parallel. We formally define the *connection graph* as follows:

Definition 5 (Connection Graph). *A connection graph is an undirected graph $G = (V : E)$, where each $v \in V$ represents an object. An edge $e(s, t) = ET \in E$ contains the timestamp sequence at which s, t are in the same cluster, i.e., $\forall t \in ET, C_t(s) = C_t(t)$.*

In graph theory, a *star* of a vertex u is the the set of neighborhood vertexes of u. To utilize *star* partition, since a vertex may appear in multiple stars, some replications of vertexes are required. In order to avoid replication of edges, we use the *directed star* as follows:

Definition 6 (Directed Star). *Assign each vertex in G an ID, a direct star of a vertex s, denoted as Sr_s, is the set of incidental edges on s such that $\forall e(s, t) \in Sr_s, s < t$. We name s as the* central vertex *of Sr_s.*

By leveraging the *directed star*, we avoids replicating the edges. A *Connection graph* and *star* examples are shown in Figure 5 (a) and (b). In (a), a connection graph is formed based on the example in Figure 1. In (b), 5 stars are presented. It can be figured out that by leveraging directed star, no edges are replicated. In implementation, as show in Algorithm 3 line 4, the comparison between vertices/objects are based on the vertex/object IDs.

5.2 Apriori Mining

To systematically discover valid patterns in each star, we design the *Apriori Mining* algorithm. To describe the algorithm, we call a candidate pattern R-pattern if the size of its object set is R. Therefore, each edge in the star is effectively a 2-pattern. The intuition of Apriori mining is the observation that $(R+1)$-patterns can be generated from R-patterns and 2 patterns. Thus, we may iteratively enumerate pattern candidates with all possible sizes. In particular, initially, for each $e(s, v) = ET$, pattern $p = (\{s, v\}, ET)$ is formed. During each iteration, we generate $(R + 1)$-patterns by joining R-patterns with the 2-patterns. Technically, the join between $p_1 = (O_1 : T_1)$ and $p_2 = (O_2 : T_2)$ generates a new pattern $p_3 = (O_1 \cup O_2 : T_1 \cap T_2)$. Note that in Sr_s, each R-pattern contains the object s, thus the join only grow a R-pattern at most to a $(R+1)$-pattern. Our mining algorithm stops where no further patterns are generated. The algorithm is illustrated as in Algorithm 4.

An illustration of Algorithm 4 is shown in Figure 5 (c). As shown, the star $Sr_3 = \{3, 4, 5, 6\}$ initially generate three 2-candidates. At every iteration, higher level candidates are generated by joining lower level candidates. When no more candidates can be generated, the algorithm stops by outputting the valid patterns.

It is notable that, in star partition, original data is replicated for $O(|\mathbb{O}|)$ times as each object may be sent to $O(|\mathbb{O}|)$ stars. Since in reality, $|\mathbb{T}| \gg |\mathbb{O}|$, the star partition is more scalable than the temporal replication. In later sections, we will describe several engineering level optimization to further reduce the amount of replicated data.

5.3 Analysis of SPM

The analysis of SPM contains two parts. We first prove the correctness of SPM. Then, we analyze the work load distribution of the star sizes.

5.3.1 Correctness

Although star partition is performed based on the connection graph, each star is indeed a projection of original
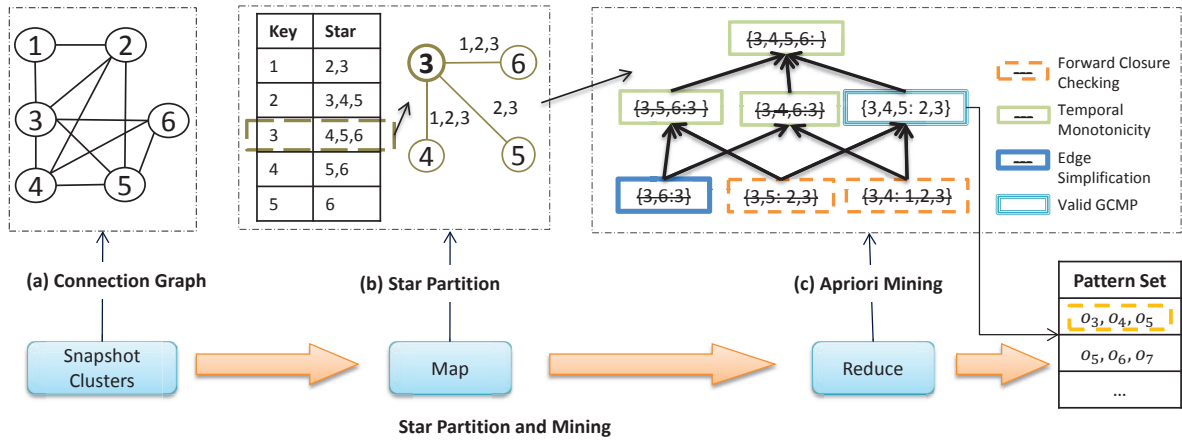
Figure 5: Star partition and mining. (a) Conceptual connection graph from Figure 1.(b) Five star partitions are generated (c) Apriori Mining with various pruning techniques.

Algorithm 4 Apriori Mining

Require: Sr_s
1: Lv ← {},Ground ← {}, Output ← {}
2: **for all** $e(s,t) = T \in Sr_s$ **do**
3:      Simply $e(s,t)$ ▷ Edge Simplification
4:      Ground.add($\langle \{s,t\},T \rangle$)
5:      Lv ← Ground
6: **end for**
7: **while** Lv is not empty **do**
8:      Lv ← Lv ⊕ Ground
9:      Remove false patterns in Lv   ▷ Temporal Monotonicity
10:      **if** union of Lv is a valid patter **then**
11:          output.add(Lv)   ▷ Forward Closure
12:          break
13:      **end if**
14: **end while**
15: output.addAll(Lv)
16: **return** output

---

trajectories. To see this, each vertex can be viewed as an object. The timestamps of center vertex s is the union of all the edges in Sr_s. The timestamps of vertex $v \neq s$ is the edge $e(s,v)$. Therefore, stars can be viewed as a trajectory database, where GCMP can be similarly defined. Using the same notions as Definition 4, we state the correctness of star partition as follows:

Theorem 2 (Soundness and Completeness of Star Partition). *Star partition is sound and complete.*

Proof. For the soundness, if P is a valid pattern in Sr_s, then at every time t, $\forall o_1, o_2 \in P.O$, $C_t(o_1) = C_t(o_2)$. By definition, P is valid in the original trajectories. For the completeness, if P is a valid pattern in original trajectories, let s be the object with smallest ID in $P.O$. Based on the definition of GCMP, $\forall t \in P.T$, $\forall o \in P.O$, $C_t(s) = C_t(o)$. It follows that all object $o \in P.O$ are in Sr_s. Furthermore, every timestamp in $P.T$ is included in Sr_s. Therefore, P is a valid pattern in Sr_s. □

5.3.2   Optimal Star Partition

An important concern in design parallel algorithms is the distribution of work loads. Traditionally, the quality of a partition strategy is measured based on two aspects: (1) the number of result partition, which affects the maximum parallelism (2) the size balance of partitions, which affects the finishing time of a job. Unlike TRM where each partition contains equal-sized snapshots, the size distribution of stars in SPM remains unknown. Nevertheless, we notice that, in SPM, the total sizes of stars are invariant. Therefore, the quality of a star partition can be formalized as the *skewness*, which is the maximum star size among all stars. Smaller *skewness* naturally results in more partitions and less imbalance.
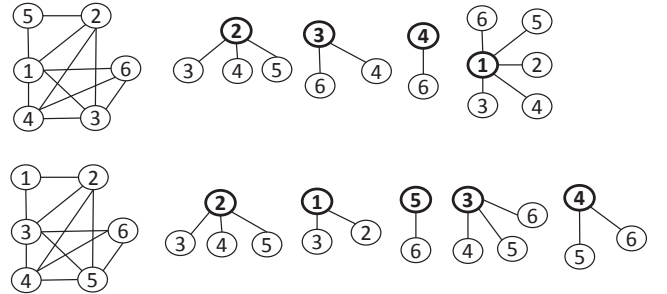

Figure 6: An alternative numbering and partitioning of the connection graph in Figure 5.

Interestingly, we note that the *skewness* of star partition is affected by the way the vertexes are numbered in the connection graph. For example, Figure 6 gives two valid numbering of vertexes of the same connection graph, but produces two different set of stars. The upper partitioning constructs 4 stars with the maximum star consisting of 5 edges. The lower partitioning constructs 5 stars with the maximum star consisting of 3 edges. Apparently the upper partitioning is inferior because its *skewness* is 5 while the lower one's *skewness* is 3.

Ideally we wish to find a numbering scheme of connection graph that minimize the *skewness*. To quantify, we use an linear algebra model as follows: Let G denote a connection graph. Let $\mathbb{A}$ be an arbitrary numbering of vertexes in G.

Let $(A : a_{i,j})$ be a boolean assignment matrix wrt. $\mathbb{A}$ (i.e., $a_{i,j}$ indicates whether vertex j is included in Sr_i). Let vector $\vec{b}$ be the *one*[1] vector. Let $\vec{c} = A\vec{b}$, then each $c_i \in \vec{c}$ denotes the size of the star Sr_i. Therefore, minimizing the *skewness* can be formulated as follows:

$$\mathbb{A} = \text{argmin}(||A\vec{b}||_\infty), \text{where } ||A\vec{b}||_\infty = \max_{1 \le j \le n}(c_j) \quad (2)$$

It is challenging to directly optimize the above equation. First, suppose there are n vertexes in G, enumerating all possible $\mathbb{A}$s leads to $n!$ combinations. Such a high complexity is trivially unpractical. Second, since G is only conceptual at runtime, the load planning cannot be done beforehand. Despite these challenges, we observe that there is a $O(1)$ time solution which is good enough as stated in the following theorem.

Theorem 3 (Balance of Star Partition). *Let G be a connection graph with n vertexes and the average degree d. Let $\mathbb{A}^*$ be the optimal numbering wrt. Equation 1. For an random numbering, $\mathbb{A}$, with high probability, the absolute skewness difference between $\mathbb{A}^*$ and $\mathbb{A}$ is $O(\sqrt{n \log n})$. That is, it is very likely that $||\mathbb{A}\vec{b}||_\infty = ||\mathbb{A}^*\vec{b}||_\infty + O(\sqrt{n \log n})$.*

Proof. Let $\mathbb{A}^*$ be the optimal numbering wrt Equation 1. Since we have a star for each object, by the degree-sum formula and pigeon-hole theorem, $||A^*\vec{b}||_\infty \ge d/2$. Next, let $e_{i,j}$ be an entry in the adjacent matrix of G. Note that edges in G are independent. Let d_i denote the degree of vertex i in G. It follows that $E[d_i] = E[\Sigma_{1 \le j \le n} e_{i,j}] = d$. Since in the star partition, each edge is assigned to the vertex with smaller IDs, the connection between $a_{i,j}$ and $e_{i,j}$ can be written as:

$$a_{i,j} = \begin{cases} e_{i,j}, i > j \\ 0, otherwise \end{cases}$$

There are two observations made on the above equation. First, since $e_{i,j}$s are independent, $a_{i,j}$s are independent. Second, since $i > j$ and $e_{i,j}$ are independent. $E[a_{i,j}] = E[e_{i,j}]E[i > j] = E[e_{i,j}]/2$.

By definition, $c_i = \Sigma_{1 \le j \le n} a_{i,j}$, is a sum of n independent 0-1 variables. Taking expectation on both sides, we get: $E[c_i] = E[\Sigma_{1 \le j \le n} a_{i,j}] = E[\Sigma_{1 \le j \le n} e_{i,j}]/2 = d/2$. Let $\mu = E[c_i] = d/2$, $t = \sqrt{n \log n}$, by Hoeffding's Inequality, the following holds:

$$Pr(c_i \ge \mu + t) \le \exp(\frac{-2t^2}{n})$$
$$= \exp(-2 \log n) = n^{-2}$$

The first step is due to the fact that all $a_{i,j}$ are bounded in the range of [0,1]. Next, since the event $(\max_{1 \le j \le n}(c_j) \ge \mu + t)$ can be viewed as $\cup_{c_i}(c_i \ge \mu + t)$, by Union Bound, we achieve the following:

$$Pr(||A\vec{b}||_\infty \ge \mu + t) = Pr(\max_{1 \le j \le n}(c_j) \ge \mu + t)$$
$$= Pr(\cup_{c_i}(c_i \ge \mu + t))$$
$$\le \Sigma_{1 \le i \le n} Pr(c_i \ge \mu + t)$$
$$= n^{-1} = 1/n$$

---
[1] Every element in $\vec{b}$ is 1

Substitute back t and μ, we achieve the following concise form:

$$Pr(||A\vec{b}||_\infty \ge (d/2 + \sqrt{n \log n})) \le 1/n$$

This indicates that, the probability of $(||A\vec{b}||_\infty - d/2)$ being less than or equal to $O(\sqrt{n \log n})$ is $(1 - 1/n)$. With the observed fact that $||A^*\vec{b}||_\infty \ge d/2$, we conclude that with probability greater than $(1 - 1/n)$, the difference between $||A\vec{b}||_\infty$ and $||A^*\vec{b}||_\infty$ is less than $O(\sqrt{n \log n})$. □

In fact, we have a tighter bound of $||A\vec{b}||_\infty - ||A^*\vec{b}||_\infty$ if the connection graph is *dense*. Specifically, if $d \ge \sqrt{12 \log n}$, the following equation holds:

$$Pr(||A\vec{b}||_\infty \ge (d/2 + O(\sqrt{d \log n}))) \le 1/n$$

Utilizing Theorem 3, in SPM, it is safe to choose the object IDs as the vertex number. This because in reality, object IDs are often hashed and can be deemed as random.

6. OPTIMIZING SPM

In Algorithm 4, there are two major factors affecting the performance. First, the edges in Sr_s affects the initial size of 2-patterns. Second, the candidates generated in each level affects the join performance. In this section, we describe several practical techniques to boost the performance.

6.1 Edge Simplification

Each edge $e(s, v)$ in Sr_s contains a time sequence ET which represents the co-occurrence of s and v. We notice that the edge between s and v is not always necessary. For example, if an edge has a cardinality less than K, it is unnecessary to include this edge to Sr_s since it cannot contribute to any patterns. This motivates us to simplify the edges in Sr_s.

Our intuition is thus to, remove the unnecessary timestamps among the edges in a star, such that the valid patterns would not be affected. To realize this idea, we formally design the concept of *candidate sequence* as follows:

Definition 7 (Candidate Sequence). *Given the pattern parameters: L, K, G, a sequence T is a* Candidate Sequence *if for any of its maximal G-connected sequence T', T' conforms to L, K.*

For example, let $L = 2, K = 4, G = 2$, sequence $T_1 = (1, 2, 4, 5, 6, 9, 10, 11, 13)$ is not a candidate sequence since one of its maximal 2-connected sequence $(9, 10, 11, 13)$ does not conform to L. In contrast, sequence $T_2 = (1, 2, 4, 5, 6, 8, 9)$ is a candidate sequence.

Not that, although T_1 is not a candidate sequence, it can be simplified to a candidate sequence (i.e, T_2). Generally, for any time sequence T, if it does not contain a *candidate sequence*, then it cannot contribute to any valid patterns. In fact, only the candidate sequence inside T affects the final patterns. Therefore, we may use the candidate sequence to simplify edges in a star. During the simplification, if an edge results in a candidate sequence of size zero, then it is removed from the star. Otherwise, the simplified edge is kept. By so doing, the size of the new star is much smaller.

We design an efficient linear time algorithm for the simplification process. It takes two rounds scan of T as shown in Algorithm 5. In the first round, the consecutive portions of T with size less than L are removed. In the second round,

the maximal G-connected sequences of size less than K are removed. Clearly the simplification algorithm takes $O(T)$ time.

Algorithm 5 Edge Simplification

Require: T
 1: —L Phase—
 2: $c \leftarrow 0$
 3: **for** $i \in (0, ..., |T|)$ **do**
 4:      **if** $T[i] - T[i-1] > 1$ **then**
 5:          **if** $i - c < L$ **then**
 6:              T remove $[c:i]$
 7:          **end if**
 8:          $c \leftarrow i$
 9:      **end if**
10: **end for**
11: —G-K Phase—
12: $s \leftarrow 1, c \leftarrow 0$
13: **for** $i \in (0 : |T|)$ **do**
14:      **if** $T[i] - T[i-1] > G$ **then**
15:          **if** $s < K$ **then**
16:              T remove $[c:i]$
17:          **end if**
18:          $c \leftarrow i, s \leftarrow 1$
19:      **else**
20:          $s++$
21:      **end if**
22: **end for**

Example 2. *Take $T_1 = \{1, 2, 4, 5, 6, 9, 10, 11, 13\}$ as an example of edge simplification. Let $L = 2, K = 4, G = 2$. In the first round of scan. T_1 reduces to $\{1, 2, 4, 5, 6, 9, 10, 11\}$. The consecutive subsequence $\{13\}$ is removed by $L = 2$. T_1 has two maximal 2-consecutive subsequences, which are $\{1, 2, 4, 5, 6\}$ and $\{9, 10, 11\}$. Since $K = 4$, $\{9, 10, 11\}$ is removed from T_1 in the second round of scan. Therefore, T_1 is simplified to $\{1, 2, 4, 5, 6\}$, which is shortened 44%.*

6.2 Temporal Monotonicity

In Apriori, we repeatedly join candidate patterns with different sizes. We observe that traditional monotonic property of Apriori algorithms **does not** hold in GCMP mining. Specifically, given two candidates P_1, P_2, if $P_1.O \subset P_2.O$ and P_1 is not a valid pattern, then P_2 may or may not be a valid pattern. However, we notice that we may form another monotonic property based on the *candidate sequence*.

The intuition is that if a candidate $P_1.T$ cannot be simplified to a *candidate sequence*, then P_1 cannot be valid pattern. Furthermore, any candidate P_2, with $P_1.O \subset P_2.O$ cannot be a valid pattern. This *temporal monotonic property* is explicitly described as in the follow theorem:

Theorem 4 (Temporal Monotonicity). *Given the temporal parameters L, G, K, for a candidate pattern P, if $P.T$ cannot be simplified to a candidate sequence, then, for any candidate P' with $P.O \subseteq P'.O$, P' cannot be a true pattern.*

Proof. Let P_1, P_2 be two candidates with $P_1.O \subseteq P_2.O$. It is easy to see that $P_1.T \supseteq P_2.T$. Suppose $P_1.T$ cannot be simplified to a candidate sequence. Then by proof of contradiction, any subset of $P_1.T$ cannot be simplified. It

follows that $P_2.T$ cannot be simplified to a candidate sequence. In summary, if $P_1.T$ cannot be simplified, P_2 can be pruned. $\square$

6.3 Forward closure checking

Although leveraging *temporal monotonicity* could largely prune false candidates and reduce the apriori search space, it is ineffective when a *true* pattern exists. In an extreme case, if a final pattern of a star Sr_s is the *union of all vertices* in the star, then in apriori, $\binom{|Sr_s|}{i+1}$ candidates needs to be generated at each level i. This results in an exponential search space while the output only contains one pattern. Generally, when candidates at level i collectively forms a true pattern, running aprior produces many wasted candidates.

Let Lv_i be the set of candidates at level i of Algorithm 4, we use the *forward closure* FC_i to denote the union of the objects in all candidates in Lv_i. Then, the *forward closure checking* is stated as follows:

Theorem 5 (Forward Closure Checking). *Let Lv_i be the candidates generated at level i in Algorithm 4, if FC_i is a proper pattern, then it is safe to terminate Algorithm 4 and directly output FC_i.*

Proof. We prove by contradiction. Suppose there exists another pattern P such that $P.O \neq FC_i$, let $X = P.O - FC_i \neq \emptyset$. Consider a subset P_1 of P which contains X with size $i+1$, (i.e., $P_1 \subseteq P, P_1 \subseteq X, |P_1| = i+1$). Since P is a proper pattern, then P_1 is also a proper pattern. Therefore $P_1 \in Lv_i$. It follows X is in the forward closure of FC_i, (i.e., $X \in FC_i$), which contradicts with $X \notin FC_i$. $\square$

It is notable that, as the level grows in Algorithm 4, the closure FC reduces, thus the pruning power of FC would be stronger. We give hybrid example of the three optimization as follows:

Example 3. *We use Figure 5 (c) to demonstrate the power of candidate pruning. As shown, at the initial stage, $\{3, 6 : 3\}$ is first pruned by Edge Simplification since its timestamps fails to be a candidate sequence. Subsequently, all further candidates containing $\{3, 6\}$ are pruned by Temporal Monotonicity. Then, we check the Forward Closure of remaining candidates (i.e., $\{3, 4\}$ and $\{3, 5\}$) and find $\{3, 4, 5\}$ is a valid candidate. Therefore, $\{3, 4\}$ and $\{3, 5\}$ are pruned, and $\{3, 4, 5\}$ is the output.*

7. EXPERIMENTAL STUDY

7.1 Implementation Issues

We use Apache Spark [2] as the experimental platform. Spark is one of the most popular MapReduce platform which uses in-memory cache to gain high speedup against Apache Hadoop []. Due to the direct support of MapReduce, our algorithm can be easily implemented in Spark. In order to help reproduce our experiments, we further address some implementation issues.

7.2 Experimental Setup

Our experiments run on a 9-node cluster, with Apache Yarn as the cluster manager. We use 1 node for Yarn resource manager, and use the remaining 8 nodes as executors

---

[2] http://spark.apache.org/

in Spark. In the cluster, each node is uniformly equipped with a 2.2GHz quad-core CPU with 32 GB memory. Inter-node communication is carried by the 1Gbps Ethernet. Some critical configuration of Spark is as follows:

Parameter	Value
Java Version	1.7.0
spark.driver.memory	2GB
spark.executor.cores	2
spark.executor.instances	11
spark.executor.memory	7GB
spark.master	yarn-cluster
spark.serializer	KryoSerializer

The clusters is managed by Yarn 2.7.1 and we use HDFS as the distributed storage. We prepare three real data set as follows:

- Geolife:

- ACTShopping:

- SingTaxi:

The summary of statistics are presented as in the following table:

7.3 Effectiveness of GCMP

7.4 Performance Comparison

7.4.1 Effects of clusters ϵ, $minPt$

7.4.2 Effects of pattern parameters M, L, K, G

7.5 SPM Analysis

7.5.1 Load Balance

7.5.2 Scalability

8. CONCLUSION AND FUTURE WORK

9. REFERENCES

[1] Y. Zheng, Y. Liu, J. Yuan, and X. Xie, "Urban computing with taxicabs," in *Proceedings of the 13th international conference on Ubiquitous computing*, pp. 89–98, ACM, 2011.

[2] Z. Li, B. Ding, J. Han, R. Kays, and P. Nye, "Mining periodic behaviors for moving objects," in *Proceedings of the 16th ACM SIGKDD international conference on Knowledge discovery and data mining*, pp. 1099–1108, ACM, 2010.

[3] J. Bao, Y. Zheng, D. Wilkie, and M. F. Mokbel, "A survey on recommendations in locationbased social networks. submitted to," *Geoinformatica*, 2013.

[4] X. Li, *Managing moving objects and their trajectories*. PhD thesis, National University of Singapore, 2013.

[5] J. Gudmundsson and M. van Kreveld, "Computing longest duration flocks in trajectory data," in *Proceedings of the 14th annual ACM international symposium on Advances in geographic information systems*, pp. 35–42, ACM, 2006.

[6] Y. Wang, E.-P. Lim, and S.-Y. Hwang, "Efficient mining of group patterns from user movement data," *Data & Knowledge Engineering*, vol. 57, no. 3, pp. 240–282, 2006.

[7] H. Jeung, M. L. Yiu, X. Zhou, C. S. Jensen, and H. T. Shen, "Discovery of convoys in trajectory databases," *Proceedings of the VLDB Endowment*, vol. 1, no. 1, pp. 1068–1080, 2008.

[8] Z. Li, B. Ding, J. Han, and R. Kays, "Swarm: Mining relaxed temporal moving object clusters," *Proceedings of the VLDB Endowment*, vol. 3, no. 1-2, pp. 723–734, 2010.

[9] Y. Li, J. Bailey, and L. Kulik, "Efficient mining of platoon patterns in trajectory databases," *Data & Knowledge Engineering*, 2015.

[10] J. Gudmundsson, M. van Kreveld, and B. Speckmann, "Efficient detection of motion patterns in spatio-temporal data sets," in *Proceedings of the 12th annual ACM international workshop on Geographic information systems*, pp. 250–257, ACM, 2004.

[11] Y. Zheng, "Trajectory data mining: an overview," *ACM Transactions on Intelligent Systems and Technology (TIST)*, vol. 6, no. 3, p. 29, 2015.

[12] D. Birant and A. Kut, "St-dbscan: An algorithm for clustering spatial–temporal data," *Data & Knowledge Engineering*, vol. 60, no. 1, pp. 208–221, 2007.

[13] P. Laube, M. van Kreveld, and S. Imfeld, "Finding remodetecting relative motion patterns in geospatial lifelines," in *Developments in spatial data handling*, pp. 201–215, Springer, 2005.

[14] D. H. Douglas and T. K. Peucker, "Algorithms for the reduction of the number of points required to represent a digitized line or its caricature," *Cartographica: The International Journal for Geographic Information and Geovisualization*, vol. 10, no. 2, pp. 112–122, 1973. doi:10.3138/FM57-6770-U75U-7727.

[15] J. Dean and S. Ghemawat, "Mapreduce: simplified data processing on large clusters," *Communications of the ACM*, vol. 51, no. 1, pp. 107–113, 2008.

Table 4: Statistics of data set

	Geolife	ACTShopping	SingTaxi
# objects	a	a	a
# timestamps	a	a	a
# data points	a	a	a